OPEN ACCESS Freely available online

PLOS ONE

Homology Modeling of Dopamine D_2 and D_3 Receptors: Molecular Dynamics Refinement and Docking Evaluation

Chiara Bianca Maria Platania, Salvatore Salomone, Gian Marco Leggio, Filippo Drago, Claudio Bucolo*

Department of Clinical and Molecular Biomedicine, Section of Pharmacology and Biochemistry, Catania University, Catania, Italy

Abstract

Dopamine (DA) receptors, a class of G-protein coupled receptors (GPCRs), have been targeted for drug development for the treatment of neurological, psychiatric and ocular disorders. The lack of structural information about GPCRs and their ligand complexes has prompted the development of homology models of these proteins aimed at structure-based drug design. Crystal structure of human dopamine D_3 (hD_3) receptor has been recently solved. Based on the hD_3 receptor crystal structure we generated dopamine D_2 and D_3 receptor models and refined them with molecular dynamics (MD) protocol. Refined structures, obtained from the MD simulations in membrane environment, were subsequently used in molecular docking studies in order to investigate potential sites of interaction. The structure of hD_3 and hD_{2L} receptors was differentiated by means of MD simulations and D_3 selective ligands were discriminated, in terms of binding energy, by docking calculation. Robust correlation of computed and experimental K_i was obtained for hD_3 and hD_{2L} receptor ligands. In conclusion, the present computational approach seems suitable to build and refine structure models of homologous dopamine receptors that may be of value for structure-based drug discovery of selective dopaminergic ligands.

Citation: Platania CBM, Salomone S, Leggio GM, Drago F, Bucolo C (2012) Homology Modeling of Dopamine D_2 and D_3 Receptors: Molecular Dynamics Refinement and Docking Evaluation. PLoS ONE 7(9): e44316. doi:10.1371/journal.pone.0044316

Editor: Yang Zhang, University of Michigan, United States of America

Received May 25, 2012; **Accepted** August 1, 2012; **Published** September 6, 2012

Funding: This work was supported in part by a National grant PON01-00110. Dr. Chiara B. M. Platania was supported by the International Ph.D. Program in Neuropharmacology, University of Catania, Italy. The authors wish to thank the "Consorzio Cometa" [http://www.consorzio-cometa.it/] for the computational hours. The funders had no role in study design, data collection and analysis, decision to publish, or preparation of the manuscript.

Competing Interests: The authors have declared that no competing interests exist.

* E-mail: claudio.bucolo@unict.it

Introduction

The dopaminergic systems in the central nervous system (CNS) have been extensively studied over the past 50 years [1]. Dopamine exerts its action through five distinct G-protein coupled receptors (D_{1-5} receptors), grouped in two classes, D_1-like and D_2-like receptors, that differ in their signal transduction, binding profile and physiological effects [1]. D_1-like receptors (D_1 and D_5) are principally coupled to stimulatory G_s-proteins and enhance the activity of adenylyl cyclase (AC), whereas D_2-like receptors (D_2, D_3, and D_4) are primarily coupled to inhibitory G_i-proteins and suppress the activity of AC [1].

Alternative splicing of D_2 receptor mRNA leads to generation of two isoforms: D_2 short (D_{2S}) and D_2 long (D_{2L}), which have been associated (though not exclusively) with presynaptic and postsynaptic populations of D_2 receptors, respectively [2]. The difference between these two splicing isoforms is represented by 29 amino acid residues in the III intracellular loop (3ICL), involved in the G protein coupling. The D_{2S} is mainly considered as a presynaptic receptor, whereas, the D_{2L} as a postsynaptic receptor [2], like the D_3 [3]. However, it has been suggested that D_3, in addition to the classical postsynaptic location, is also localized in the presynapse, where it modulates dopamine release and synthesis [4,5]. D_2 and D_3 receptors display a high degree of sequence homology and share the putative binding site for dopamine and synthetic ligands at the interface of transmembrane helices [6]. D_2 and D_3 receptors also share the signal-transduction mechanism, though under certain conditions the latter may exert a weaker stimulation of effectors like AC [7,8]. Several pathological conditions such as schizophrenia, Parkinson's disease, Tourette's syndrome, and hyperprolactinemia have been linked to a dysregulation of dopaminergic transmission [1]. Furthermore, D_2 and D_3 receptor have been implicated as potential target for drug development in ocular diseases such as glaucoma [9,10,11,12,13,14,15]. D_2-like receptors represent the most relevant class in the pathophysiology of neurological and psychiatric disorders. However, while D_2 receptor is considered the principal target to control the positive symptoms of schizophrenia, none of antipsychotics approved so far discriminates D_2 from D_3 receptors; on the other hand, the functional significance of D_4 receptor largely remains to be defined.

Human dopamine D_2 receptor (hD_2) and hD_3 are highly homologous [16], sharing 78% of sequence identity in the transmembrane domains [17,18], including the binding site [19]. This sequence identity has introduced difficulties in the design of selective ligands. However, in the past two decades, medicinal chemists have succeeded, by using ligand-based approaches, in developing selective agonists such as aminotetralins: 7-hydroxy-2-dipropylaminotetralin (7-OH-DPAT) [20], trans-7-hydroxy-2-[N-propyl-N(3′-iodo-2′-propenyl)amino]tetratalin (7-OH-PIPAT) [21,22] and rotigotine [23,24]. Because the pharmacokinetic profile of 7-OH-DPAT was unsatisfactory, a bioisosteric replacement of the hydroxyphenyl group was carried out [25], leading to ligands selective for D_3 over D_2 subtype: quinpirole and pramipexole [26]. More recently a compound with the pyrazole moiety of quinpirole, FAUC 329, was found to selectively activate D_3 receptor [$K_i = 4.3$ nM] over D_2 receptor and it has a partial agonist activity (52% compared to quinpirole) [27]. Other drug

design studies were carried out successfully by Lopez et al [28] who reported benzolactam derivatives with distinct selectivity against D_3 and D_2 receptors; functionalized benzolactam compounds were reported to have D_3 dopaminergic agonism [29]. Recently, Tschammer et al [30] synthesized heterocyclic dopamine surrogates, among which one compound (biphenylcarboamide (S)-5a) has a very high affinity (27 pM) at the D_3 receptor and high selectivity over D_2 subtype.

The crystal structure of hD_3 has been solved [31] and identified as a powerful tool for structure-based drug discovery of selective dopaminergic D_2-like ligands [32]. This crystallized receptor is a hD_3-lysozyme chimera, where the 3ICL is replaced by the lysozime protein; moreover, the receptor bears the mutation Leu119Trp in order to increase the thermal stability of the system. Recently, the determination of the crystal structure of hD_3 receptor and subsequent efforts in molecular modeling led to successful prediction of the pose of eticlopride in complex with a refined homology model of D_3 receptor [33]. Kortagere et al [34] analyzed in 2011 the binding mode of preferential D_3 ligands by means of site-directed mutagenesis and homology modeling studies (template structure 2RH1); these authors identified Ser 192 of V helix as an important site of interaction for the activation of D_3 receptor. Ser 192 belongs to a cluster of three serine residues (Ser 192, Ser 193, Ser 196); thus we have carefully looked at these residues, and their homologous (Ser 193, Ser 194, Ser 197) in hD_{2L} subtype, in our docking protocol. The subtype selectivity of D_2-like ligands had been also studied before, by Wang et al [35], in the absence of structural information on D_3 and D_2 receptors, by a mixed structure-based (homology modeling using β_2-adrenergic and rhodopsin receptors, molecular dynamics of haloperidol-receptor complexes) and ligand-based approach (3D-QSAR). These authors, however, did not carry out docking calculations. No study published so far has used a total structure-based approach for modeling ligand interactions with the hD_3 and hD_{2L}. In the present study we aimed at building and validating homology models of hD_3 and hD_{2L} receptors using the hD_3 receptor structure (3PBL) as template. Furthermore, in order to better discriminate their structural difference as well as selective ligands, we have carried out a structural optimization by molecular dynamics (MD) simulations of these two receptors for 3 ns in an explicit palmitoyl-oleoyl-phosphatidyl-choline (POPC) bilayer, that mimics the plasma membrane lipid environment, reaching a structural differentiation of these homologous receptors. The short-term MD simulations were adequate to obtain optimized structures of hD_3 and hD_{2L} receptors, because of the high homology and sequence identity between target and template proteins. We have validated these optimized structures using a total structure-based approach by molecular docking calculations that are extremely influenced by the reliability of receptor structure. The validation of optimized structure models was successful, giving good correlation between experimental and predicted K_i of agonists.

Methods

Homology Modeling

The retrieved (Swiss-Prot) protein sequences of hD_3 and hD_{2L} receptors are respectively: P35462.2 and P14416.2. Homology models of hD_3 and hD_{2L} receptors were obtained by the Automated Modeling tool of Swiss Model web service http://swissmodel.expasy.org/[36,37] using the crystal structure of the human D_3 dopaminergic receptor-lysozyme chimera (Protein Data Bank-code 3PBL) in complex with the antagonist eticlopride as template. N-terminals of receptors were not modeled, because we focused on the binding pocket. Moreover the structure of N-terminal of hD3 was not solved by Chien et al [26]. The terminal residues Tyr 32 in hD3 and Tyr 37 in hD_{2L} were blocked in the homology models by acetylation. The hD_3 model was validated by docking eticlopride in the binding pocket. The model validation was carried out using two different molecular docking software (the docking protocol is reported in the Docking section): Autodock Vina (Vina) and Autodock 4.2 (AD4.2).

Molecular Dynamics

Homology models of dopaminergic receptors were embedded in a pre-equilibrated POPC bilayer. Then, the systems were hydrated with TIP3P water molecules, and neutralized adding NaCl up to 150 mM. CHARMM 27 parameters were assigned to all molecules. Disulfide bridges of hD_3 were parameterized by involving the following residues: Cys 103-Cys 181 connecting the III helix with the II extracellular loop (2ECL) and Cys 355-Cys 358 in the 3ECL. In the hD_{2L} model we parameterized the conserved disulfide bridge between the III helix and 2ECL involving the Cys 109-Cys 187 residues. The system preparation processes (building of bilayer, embedding of the proteins into the membrane, hydration and neutralization) were done using VMD v1.8.7 [38]. Before MD simulations the systems were equilibrated as follows: i) MD of lipid tails for 50 ps (time-step = 1 fs) while protein, water, ions and lipid head groups were kept fixed; ii) equilibration for 100 ps (time-step = 1fs) of water-ions-lipids, while proteins were kept fixed by applying harmonic constraints; iii) 500 ps (time step = 1 fs) of system equilibration, with no constraints applied to molecules. After the described steps of equilibration, 3 ns of MD simulation were carried out with time-step of 2 fs, collecting trajectory data every 10 ps. The SHAKE algorithm, which constraints the hydrogen-heavy atom bonds.was applied. Equilibration steps and simulations were carried out using NAMD v2.7 [39]. Langevin dynamics and piston were used to maintain constant temperature (300 K) and pressure (1 atm) during simulation. The area per lipid was maintained constant, after the equilibration steps (NPAT ensemble). The particle number of systems was 83242 for hD_3-lipids-water-ions and 83429 for hD_{2L} in membrane. Periodic Boundary Conditions (PBC) and Particle Mesh Ewalds (PME) method [40] were used to treat long-term electrostatics (time-step of 4 fs). The cut-off at 10 Å was applied to Van der Waals and coulombic interactions and switching functions started at 9 Å. First stage minimization was performed using the steepest descent algorithm whereas the conjugate gradient was used during production runs.

Docking and Virtual Screening

We carried out two different molecular docking studies using Vina and AD4.2 software. Vina [41] is an accurate algorithm faster than AD4.2; for this reason it was used for docking calculation of a large group of D_2-like ligands and for virtual screening study. AD 4.2 [42] provided the best prediction of pose of eticlopride in the hD_3 homology model, thus we have chosen it for accurate docking calculation such as prediction of K_i of well-known D_2-like agonists docked into the refined homology models of hD_3 and hD_{2L} receptors. File preparation for AD4.2 docking calculations was carried out using the AutodockTool (ADT), a free graphics user interface (GUI) of MGL-tools.

The search space for all docking calculations included the orthosteric binding pocket individuated by eticlopride in 3PBL, the allosteric binding pocket reported by Chien et al [31] and the extracellular domain of receptors. An high exhaustiveness, 32, was used in Vina calculation because the search space applied to hD_3 and hD_{2L} receptor is relatively wide. In calculations carried out

with AD4.2 we chose, as search algorithm, the time-consuming Lamarkian genetic algorithm (GA), that generated the best docking results for eticlopride in hD_3 homology model. Hundred iterations of GA with 2,500,000 energy evaluations per run were carried out. Population size was set to 150 and a maximum of 27,000 generations per run was carried out, followed by automatic clusterization of poses. Top scored (lowest energy) and more populated poses with orthosteric binding, as reported by Kortagere et al [34],were selected for analysis of ligand-protein interactions using the GUI ADT. AD 4.2 uses a semi-empirical free energy function and a charge-based method for desolvation contributes; the free energy function was calibrated using a set of 188 structurally known ligand-complexes with experimentally determined binding constants [43]. The binding energy of ligand poses (Kcal/mol) is the sum of intermolecular energy, internal energy of the ligand and torsional free energy minus the unbound-system energy (see in Supporting Information S1 about the calculation of K_i from AD4.2 binding energy values and Supporting Information S2 for ligand poses and optimized structure of receptors).

Ligand Dataset

Structure files of ligands were retrieved from PubChem [44], ZINC database [45], and, when not available there, from PRODRG web service (http://davapc1.bioch.dundee.ac.uk/prodrg/), as.mol2 files [46]. Whenever a conversion of file format was necessary it was done by Open Babel [47]. Protonation state of ligands was assigned at pH = 7.4. Three replicas of dockings were carried before and after MD simulations in order to assess the structure differentiation of homology model simulated in membrane. The following ligands were used in fast docking calculations with Vina: r-7-OH-DPAT, s-7-OH-DPAT, r-7-OH-PIPAT, s-7-OH-PIPAT, bromocriptine, lergotrile, lisuride, pergolide, cianergoline, cabergoline, SDZ-GLC-756, PD128907, pramipexole, rotigotine, ropinirole, eticlopride, U99194A, Ru24213, GR103691, r-GSK89472, s-GSK89472, s-nafadotride, NGB2904, PG01037, PNU177864, SB-269-652, S33084, SB277011A, S14297, S17777 and compounds of the USC series from Ortega et al [29] (USC-A401, USC-B401, USC-H401, USC-I401, USC-K401, USC-M401). The D_3 agonists, represented in Figure 1, r-7-OH-DPAT, r-7-OH-PIPAT, pramipexole, ropinirole, rotigotine, quinpirole, dopamine, PD128907 and cis-8-OH-PBZI (cis-8-hydroxy-3-(n-propyl)1,2,3a.4,5,9b-hexahydro-1H-benz[e]indole) were docked with AD4.2 into the hD_3 and hD_{2L} receptors optimized by MD; the predicted K_i values were correlated to the experimental ones. Eighty nine compounds, retrieved from ZINC database, were used to build a small focused drug-like database of ligands (according to the Lipinski's rule of five and similar at 70% to pramipexole); they were docked with Vina into hD_3 and hD_{2L} refined receptors. Structural alignments of proteins and figures were done with the molecular visualization software Open PyMOL. All software utilized in our study were open source or under free of charge academic license. Computational hours were provided by the GRID service "Consorzio Cometa" [http://www.consorzio-cometa.it/].

Results

Homology Modeling

We built the homology models of hD_3 and hD_{2L} receptors. Two disulfide bridges were modeled in hD_3 receptor according to the crystal structure 3PBL [31], the canonical one that connect the 2ECL with the III helix and the disulfide bridge in the 3ECL involving residues Cys 355 and Cys 358. In hD_{2L} receptor only the conserved disulfide bridge was modeled, because we considered that a single residue of distance between the two conserved cysteine residues (Cys 399 and Cys 401) may lead to unstable disulfide bond. Validation for the hD_3 model, by docking eticlopride with Vina and AD4.2 was performed. Both software were able to reproduce the eticlopride conformation in the binding pocket; AD4.2 gave the lowest root mean square deviation (RMSD, 0.4 Å) and better reproduced the internal H-bonds (Figure 2A), compared to VINA (Figure 2B), that gave 0.6 Å RMSD for re-docked eticlopride. We have evaluated the similarity of hD_3 and hD_{2L} homology models by means of structural alignment. The tridimensional alignment revealed that the two homology models did not differ in transmembrane core structure (Figure 3A), as expected from their high sequence identity; furthermore, RMSD between the two aligned GPCRs was very low (0.033 Å). We have, further, analyzed the structural similarity and capacity of discrimination of active D_2-like ligands by fast docking calculations, with the Vina docking software. The structure similarity was reflected by the high correlation ($R^2 = 0.91$, Figure 3C) of predicted binding energy of D_2-like ligands docked into the homology models of hD_3 and hD_{2L}. Thus, these two homology models do not seem useful, without a structural refinement, for virtual screening directed at the recognition of selective ligands.

Molecular Dynamics

We have simulated for 3 ns the hD_3 and hD_{2L} homology models in a water-membrane environment that reproduces the biological milieu where these two GPCRs are located, to further discriminate their structural difference. By reporting the RMSD of protein structure from the starting homology model, both receptors differentiate in structure and reach a relative stable conformational minimum roughly after 1.25 ns (Figure 4). Total energy (E_{tot}) and potential energy (E_p) of systems are constant during the MD simulation (Supporting Information S1) and energy values of D_3 receptor are slightly lower compared to the energy of D_{2L} subtype. We stopped simulations at 3 ns because we reached stable local minima and distinct conformations for hD_3 and hD_{2L} receptors. Longer simulations (over 30 ns) might reveal other local minima and further characterize the conformational space of these receptors; this goal, however, is beyond the aim of our study. GPCRs are in equilibrium between active and inactive conformation, and, as far as the inactive conformation is concerned, a structural marker, the "ionic lock" was described in several studies [48,49,50,51] and was also revealed in the crystal structure of eticlopride-hD_3 complex (3PBL) [31]. This ionic lock involves, four conserved residues, Arg128-Asp127-Glu324-Tyr138 in hD_3 (Figure 5A), and Arg132-Asp131-Glu368-Tyr142 in hD_{2L} receptor (Figure 5B), respectively. The salt-bridges that constitute the ionic lock are retained during the 3 ns of simulation. We can assume that the conformation of receptors, that reached the relative minimum, describes the inactive state. The superimposition of the simulated hD_3 and hD_{2L} receptors confirmed the structural deviation of receptors in membrane, as the RMSD was 1.63 Å (Figure 3B). The differentiation of the two homologous receptors was further strengthen by the lower correlation ($R^2 = 0.74$) of binding energies of D_2-like ligands docked, with VINA, into hD_3 and hD_{2L} optimized structures (Figure 3D). We have measured the Cα deviation of residues belonging to the orthosteric binding pocket of receptors in order to further characterize the structural modification of hD_3 and hD_{2L} induced by the membrane environment. The deviations of these residues, comparing the initial homology models with the refined structures are reported in Table 1. The residues of binding pocket of hD_{2L}

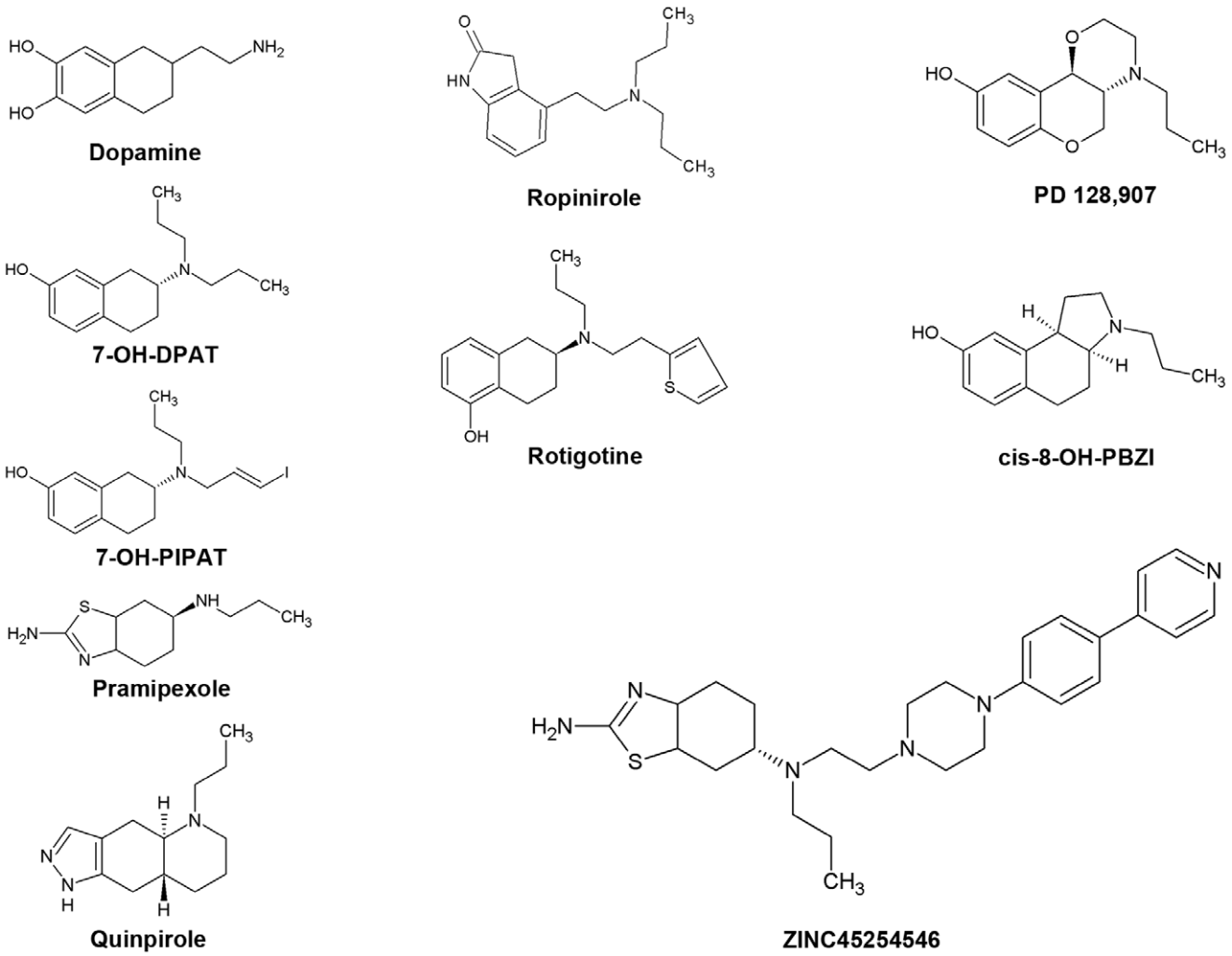

Figure 1. D_2-like agonists.
doi:10.1371/journal.pone.0044316.g001

receptor deviated from starting model more than residues of hD_3 subtype (Table 1). The V helix of hD_{2L} receptor had the greater deviation than other helices after the simulation (Supporting Information S1), involving the extracellular and intracellular side (transversal to the plane of the membrane). The VI and VII helices deviated mostly in the extracellular side and the greater deviation is shown for the VII helix (Supporting Information S1). Within the seven helices of hD_{2L} receptor, only IV helix had a major

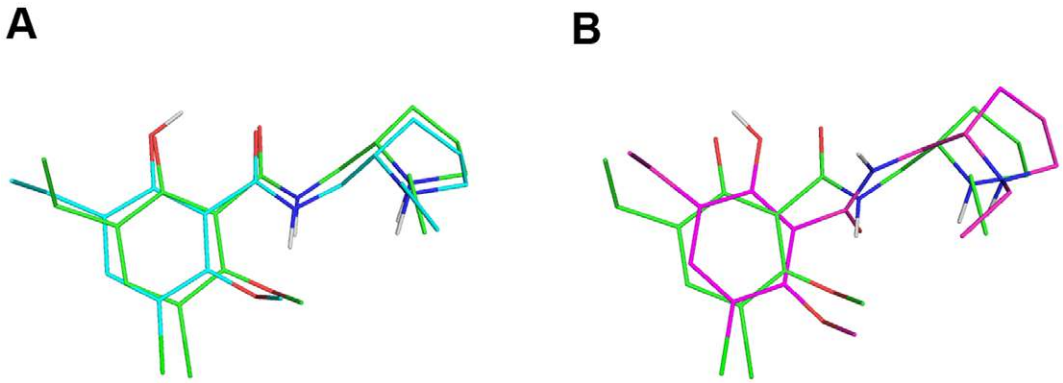

Figure 2. Re-docking eticlopride. Superimposition of eticlopride re-docked with AD4.2 (cyan lines, A) and with Vina (magenta lines, B) toward eticlopride in complex with hD_3 in the crystal structure 3PBL (green lines).
doi:10.1371/journal.pone.0044316.g002

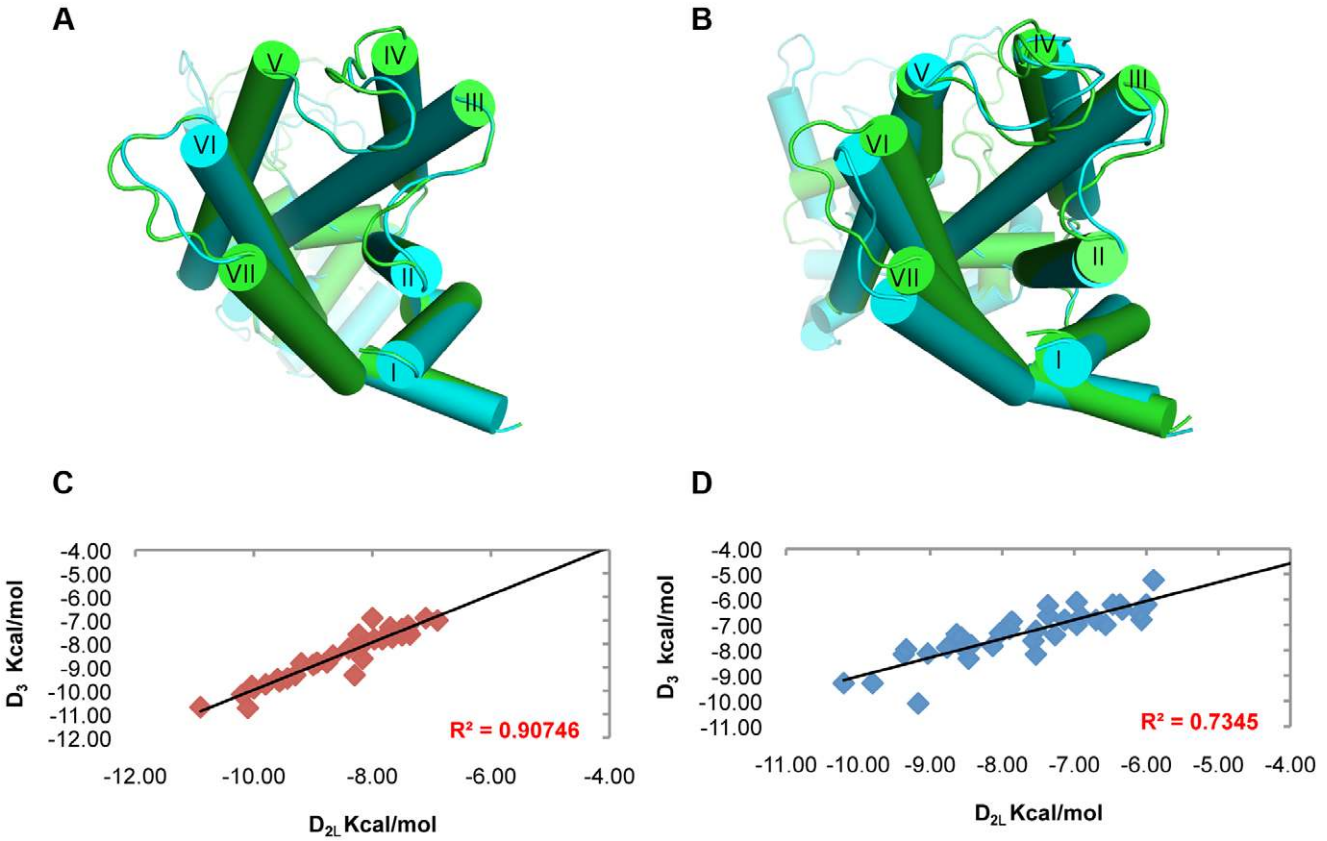

Figure 3. Structure differentiation of hD_3 and hD_{2L} receptors simulated in membrane. (A) Superimposition of hD_3 (green cartoon) and hD_2 (cyan cartoon) homology models before the refinement with simulation in membrane. (B) structural alignment of hD_3 (green cartoon) and hD_2 (cyan cartoon) receptors after 3 ns of MD simulation in membrane. (C) high correlation of hD_3 and hD_2 binding energies (Autodock Vina) of D_2-like ligands from homology models without MD refinement. (D) low correlation of hD_3 and hD_2 binding energies (Autodock Vina) of D_2-like ligands after MD refinement.
doi:10.1371/journal.pone.0044316.g003

transversal deviation and a sensible deviation along the z-axis of membrane (Supporting Information S1). Furthermore, the binding pocket of hD_3 receptor was also remodeled in membrane, because there were major structural deviations involving the residues of V helix (Ser 192, Ser 193, Ser 196), VI helix (His 349) and VII helix (Tyr 375) (Tables 1 and Supporting Information S1). We further characterized the binding pocket of hD_3 and hD_{2L}, before and after refining with MD simulations, by using the web service fpocket http://fpocket.sourceforge.net/[52]. Fpocket generates clusters of spheres to describe each pocket of a given protein; in Figure 6 we have assigned different colors to pockets of hD_3 and hD_{2L} receptors, before and after optimization. Before simulation in membrane, the binding pockets of the two receptors were very similar in shape and dimension. After simulation, the pocket of hD_3 became smaller than that of hD_{2L} and divided in three pockets (Figure 6C); the one in blue includes the orthosteric and the allosteric pockets, the one in magenta is surrounded by the extracellular loops, and the deepest and smallest pocket is colored in red. In docking calculations, we did not find poses in the red pocket, that was occupied by water molecules during MD simulation (data not shown). The pocket of hD_{2L} after simulation became bigger than that of D_3 subtype (Figure 6B and 6D). The hD_{2L} receptor after simulation shows a big pocket (orange spheres) and a smaller pocket (magenta) located along the big one, between the III and IV helices. After simulation the red pocket of hD_{2L} appears included within the orange one (Figure 6B and 6D). The optimized structures of hD_3 and hD_{2L} used for analysis and docking calculations were extracted randomly from one of the last frames of simulations that characterize the relative conformational equilibrium, by considering as equivalent frames belonging to the same local minimum. To confirm this assumption we randomly selected one additional frame from each local minimum of the hD_3 and hD_{2L} MD simulations. These two additional frames resulted equivalent to the previous, because, when carrying out docking of pramipexole superimposable results were obtained both in terms of binding energy (Table 2, values in brackets) and poses (data not shown). We did not carried out a clusterization of trajectories because we have reached one local minimum in each simulation. Furthermore, as reported by Yap et al [53] clusterization of GPCR trajectories, is not useful for selecting the representative structure to be used in docking calculation.

Docking

We validated the optimized structures of hD_3 and hD_{2L} receptors by docking D_3–preferring receptor agonists into receptor binding pockets using AD 4.2 docking software, which provided the best result of eticlopride pose prediction in the hD_3 homology model. Binding energy of agonists docked in hD_3 and hD_{2L} receptors correlates with their higher affinity for the D_3 subtype (Table 2), consistent with more polar contacts of ligands docked into D_3 receptor compared to ligands docked into the D_{2L} subtype (Table 3). The experimental pK_i values (retrieved from http://

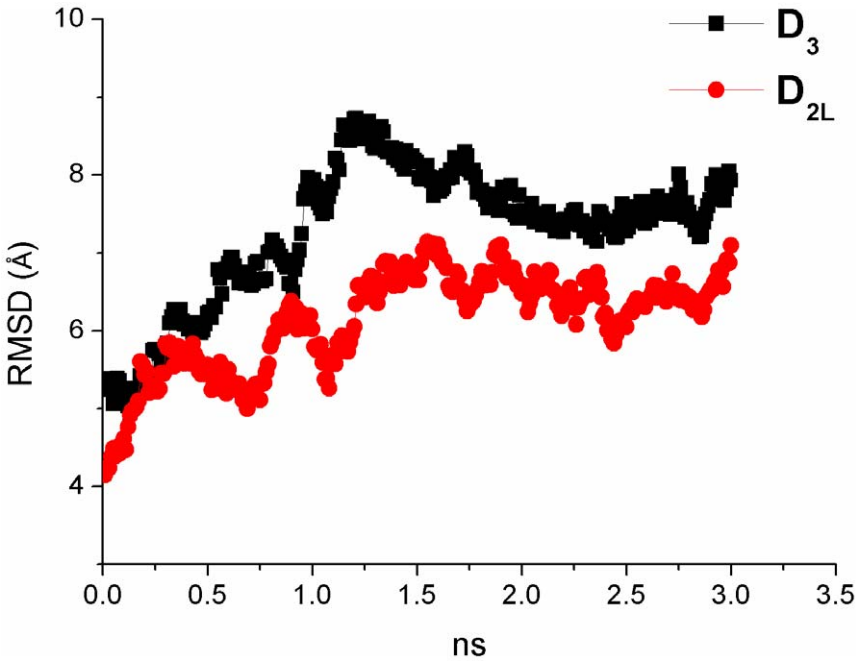

Figure 4. Analysis of Root Mean Square Deviation of Cα atoms during molecular dynamics simulation. RMSD respect to the starting structures, homology models, of hD_3 (black squares) and hD_{2L} (red circles) receptors.
doi:10.1371/journal.pone.0044316.g004

pdsp.med.unc.edu/free access database) of agonists were compared with the predicted values (Figure 7, see also Supporting Information S1) obtaining a good correlation as indicated by Pearson coefficients relative to hD_3 and hD_{2L} receptors equal to 0.88 and 0.83 respectively ($p<0.005$). Linear regression coefficients however were low (Figure 7), due to the limitations of AD4.2 in predicting absolute values of K_i, as reported by Lape et al [54] and by Yap et al [55]. Another explanation to the mentioned issue might be related to the heterogeneity in K_i determination assays. Quinpirole was not included in the regression analysis because it was an outlier, even though its predicted binding energies for hD_3 and hD_{2L} correlate with the higher affinity toward the D_3 subtype. Quinpirole is a bioisoster of DPAT, among other ligands included in the regression model (Figure 1), with a tricyclic structure where the hydroxyphenyl group is substituted with a pyrazolic group. On the contrary, PD-128907, a tricyclic compound with the hydroxyphenyl group, fits in the regression model of pK_i for hD_3 and hD_{2L} receptor. Another tricyclic compound included in the regression model is cis-8-OH-PBZI (PBZI), which retains the position of hydroxyl and amine groups of 7-OH-DPAT. The affinity of PBZI was determined for D_{2S}, D_3 and D_4 receptors but not for D_{2L} receptor, therefore we did not include it in the regression model for hD_{2L} receptor. Recently, PBZI was found to not induce tolerance and slow response termination, in comparison to known agonists such as 7-OH-DPAT and pramipexole [56]. Comparing the tricyclic structures of PD-128907, PBZI and quinpirole, this latter might behave as an outlier in the chemical space, due to the substitution of the hydroxyphenyl moiety with the pyrazol condensed group.

Virtual Screening

Pramipexole is a selective D_3 agonist ($D_2/D_3 = 75.5$) indicated in the treatment of early-stage Parkinson disease. This agonist was chosen as reference for building a small ligands database (89 molecules), where drug-like compounds are 70% similar to pramipexole. We carried out a virtual screening by docking these ligands into the refined hD_3 and hD_{2L} models. The top scored compound is a novel selective D_2-like agonist synthesized by Ghosh et al [57] (-)-(S)-N6-Propyl-N6-(2-(4-(4-(pyridin-4-yl)phe-

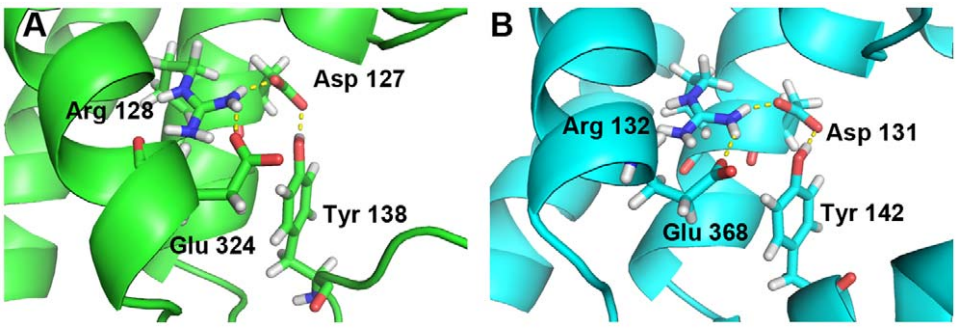

Figure 5. Ionic-look, structural marker of inactive state of G-protein Coupled Receptors. (A) hD_3 and (B) hD_{2L} receptor.
doi:10.1371/journal.pone.0044316.g005

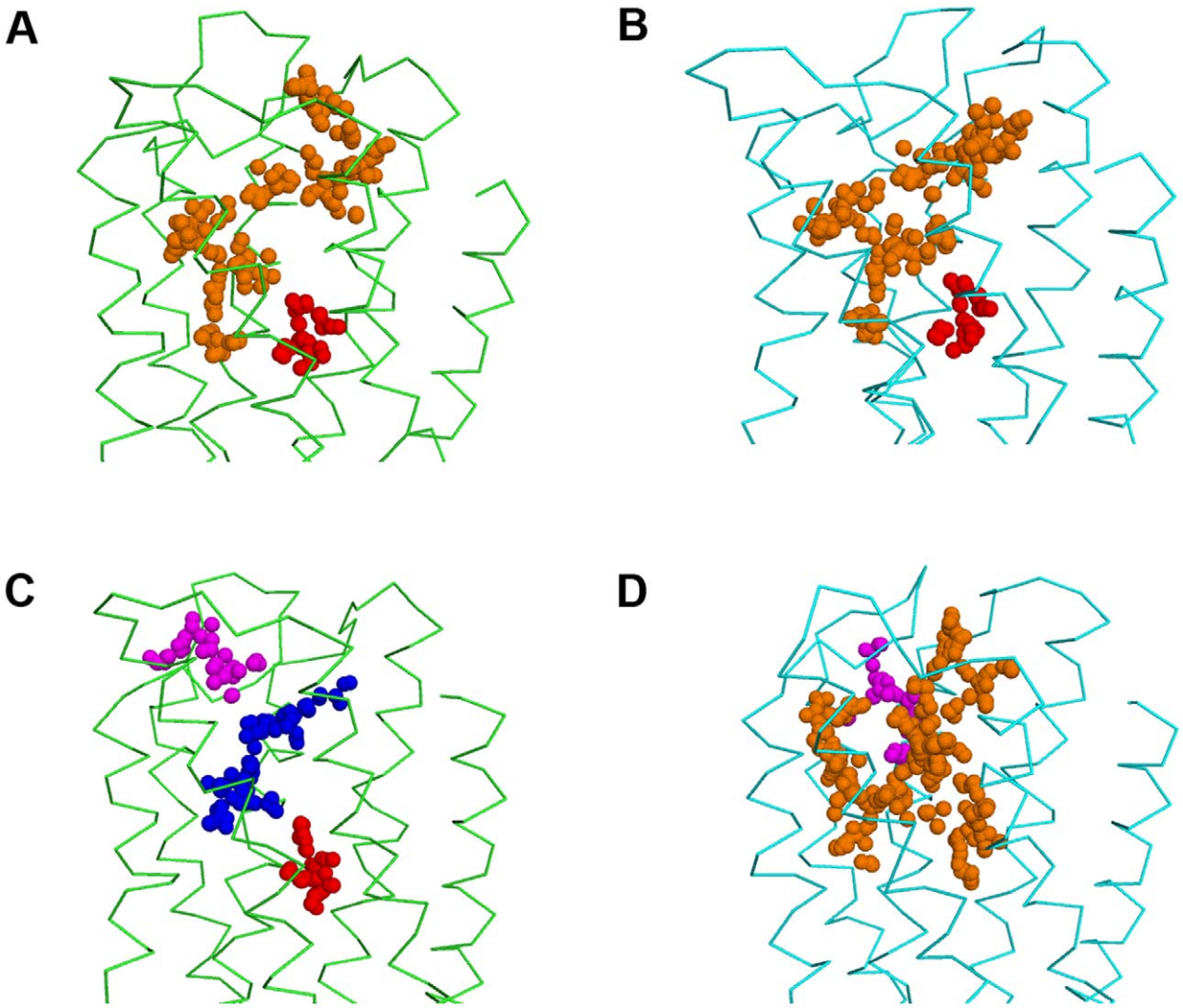

Figure 6. Evolution of binding pockets of hD_3 and hD_{2L} receptor after model refinement. Pockets generated by Fpocket server are represented as colored clusters of spheres. Left panels represent hD_3 (green ribbons) and right panels represent hD_{2L} (cyan ribbons), before (A, B) and after (C, D) MD simulations. The red circles target the orthosteric binding pocket whereas the black circles highlight the allosteric binding pocket.
doi:10.1371/journal.pone.0044316.g006

Table 1. Deviations of Cα of residues belonging to the orthosteric binding pocket of optimized receptors in comparison with the starting models.

hD_3		hD_{2L}	
Residue	**Cα deviation (Å)**	**Residue**	**Cα deviation (Å)**
Asp 110 (III helix)	0.3	Asp 114 (III helix)	1.3
Ser 192 (V helix)	0.9	Ser 193 (V helix)	1.3
Ser 193 (V helix)	0.9	Ser 194 (V helix)	1.0
Ser 196 (V helix)	1.3	Ser 197 (V helix)	3.2
Trp 342 (VI helix)	0.3	Trp 386 (VI helix)	1.5
Phe 345 (VI helix)	0.3	Phe 389 (VI helix)	1.8
Phe 346 (VI helix)	0.3	Phe 390 (VI helix)	0.9
His 349 (VI helix)	0.6	His 393 (VI helix)	1.8
Tyr 375 (VII helix)	1.2	Tyr 416 (VII helix)	0.9

doi:10.1371/journal.pone.0044316.t001

nyl)piperazin-1-yl)-ethyl)-4,5,6,7-tetrahydrobenzo[d]-thiazole-2,6-diamine, deposited in the ZINC database with the name ZINC45254546. This compound is reported to have high affinity towards hD_3 subtype ($D_{2L}/D_3 = 56.5$) (Table 4). ZINC45254546 (Figure 1) is an hybrid compound bearing a pramipexole moiety and a piperazin(4-phenyl(4pyridyl)) antioxidant group. This compound was re-docked with AD4.2, into hD_3 and hD_{2L} receptors. As shown in Figure 8, polar contacts involved aspartate and threonine residues in III helix and the cluster of serine residues in V helix that interact with the pramipexole group. The analysis of pose of ZINC45254546 did not show the H-bond with Asp114 in hD_{2L}, which may explain its lower affinity toward the D_{2L} subtype. The piperazin(4-phenyl(4pyridyl)) group interacted with part of the 2ECL in hD_3 subtype and with residues of II and VII helices in hD_{2L} receptor, that characterize the allosteric pocket. The top 30 compounds (ZINC-db code), docked into hD_3 and hD_{2L} receptors, are reported in Supporting Information S1.

Table 2. Predicted binding energy (Autodock 4.2) of D_3 agonists towards hD_3 and hD_2 receptors. Experimental K_i (exp. K_i) with respective references are also shown.

D_3 agonist [reference]	hD_3 $E_{binding}$ (kcal/mol)	hD_2 $E_{binding}$ (kcal/mol)	hD_3 exp. Ki (nM)	hD_2 exp. Ki (nM)
Dopamine	−6.5	−6.0	32.5[(1)]	598[(1)]
r-7-OH-DPAT [61]	−7.7	−6.4	1.58	158
r-7-OH-PIPAT [19]	−8.4	−7.3	2.9[(2)]	142[(2)]
Pramipexole [62]	−7.1	−6.6	10.5	790
Pramipexole[(3)]	(−7.1)	(−6.4)		
Ropinirole [62]	−7.0	−6.4	37.2	933
Rotigotine [63]	−8.4	−7.4	0.71	13.5
Quinpirole [64]	−7.6	−6.6	39	1402
PD 128907 [65]	−7.7	−6.0	3.1	1573
cis-8-OH-PBZI [66]	−7.1	ND	27.4	ND

[(1)]Average value from PDSP database: http://pdsp.med.unc.edu/indexR.html.
[(2)]The K_i is reported for the racemic 7-OH-PIPAT.
[(3)]Pramipexole re-docked in two other frames of hD_3 and hD_{2L} receptor; see also text.
doi:10.1371/journal.pone.0044316.t002

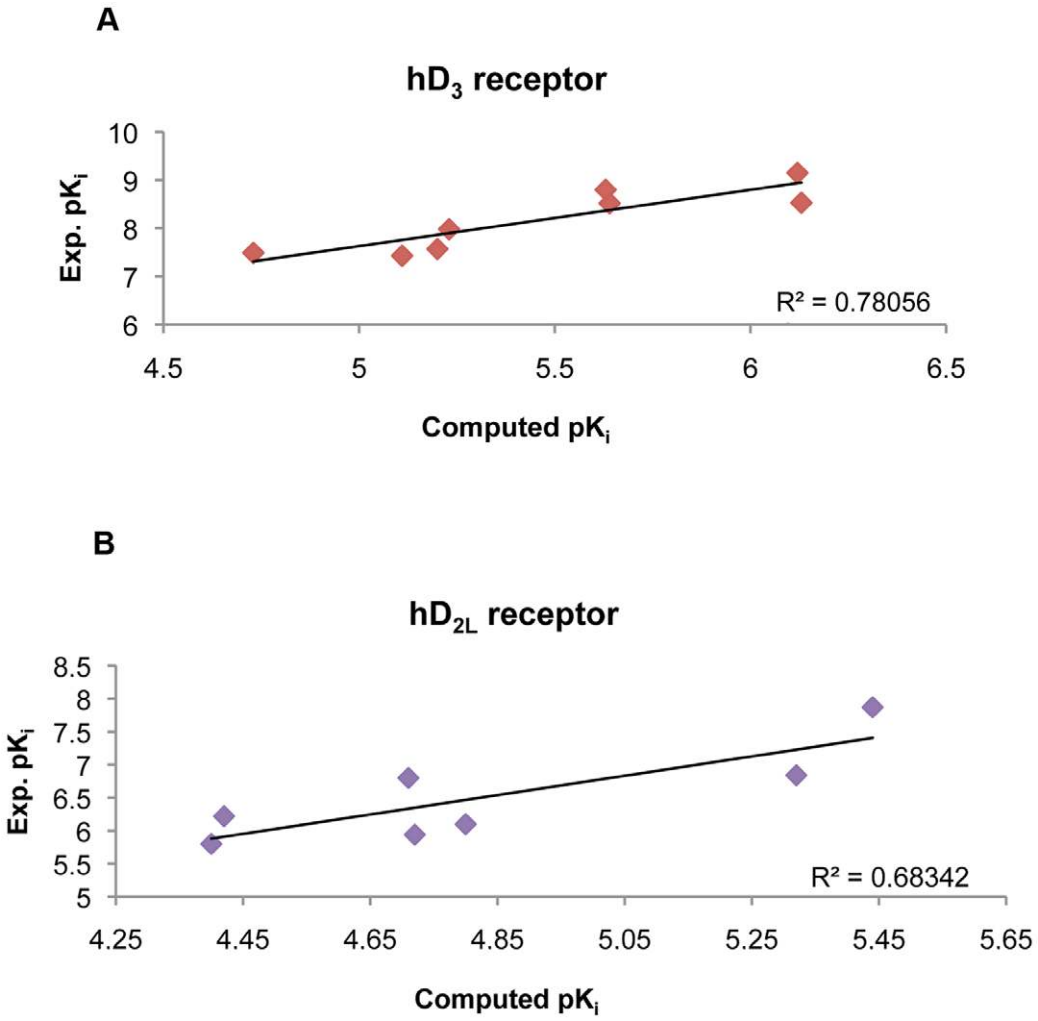

Figure 7. Correlation of predicted pK_i and experimental pK_i values. Plots of D_3 preferring agonists docked toward hD_3 (A) and hD_{2L} (B) receptors: a. dopamine; b. 7-OH-DPAT; c. 7-OH-PIPAT; d. pramipexole; e. quinpirole; f. ropinirole; g. rotigotine; h. PD 128,907; i. cis-8-OH-PBZI; j. ZINC45254546.
doi:10.1371/journal.pone.0044316.g007

Table 3. Ligand protein-interaction of D_3–preferring receptor agonists docked with AD4.2.

Ligands	hD_3		hD_{2L}	
	Hydrogen bonds-polar contacts	**Hydrophobic contacts**	**Hydrogen bonds-polar contacts**	**Hydrophobic contacts**
Dopamine	Asp 110, Thr 115, Ser 192, Ser 196.	Ile 183, Phe 345, His 349.	Asp 114, Ser 194	Val 115, His 393, Phe 389, Phe 390.
r-7-OH-DPAT	Asp 110, Ser 192, Ser 196, Thr 115.	Ile 183, Phe 345, His 349.	Asp 114,, Ser 193.	Val 111, Phe 110, Ile 184, Phe 390.
r-7-OH-PIPAT	Asp 110, Val 111 (C = O of peptide bond), Thr 115, Ser 192.	Val 111, Val 107, Ile 183, Trp 342, Phe 345, His 349.	Asp 114, Val 190 (C = O of peptide bond), Ser 193.	Val 111, Phe 110, Ile 184, Phe 390.
Pramipexole	Asp 110, Thr 115, Ser 192, Ser 196.	Val 111, Trp 342, Phe 345, Thr 369.	Asp 114, Val 190 (C = O of peptide bond), Ser 194.	Phe 110, Val 111, Phe 390, His 393.
Ropinirole	Asp 110, Ser 192	Val 189, Trp 342, Phe 345, His 349, Tyr 373	Asp 114, Ser 193.	Val 111, Phe 110, Val 115, Phe 390, His 393
Rotigotine	Asp 110, Ser 192.	Val 107, Phe 106, Phe 345, Phe 346, His 349	Asp 114	Phe 110, Val 111, Val 115, Ile 184, Phe 390, His 393
Quinpirole	Asp 110, Ser 192	Val 111, Ile 183, Trp 342, Phe 345, Thr 369, Tyr 373.	Asp 114	Val 115, Trp 386, Phe 389, Gly 415, Tyr 416.
PD128907	Asp 110, Ser 192	Val 111, Ile 183, Phe 188, Trp 342, Phe 345, Phe 346, Thr 369, Tyr 373.	Asp 114	Val 111, Phe 389, His 393.
cis-8-OH-PBZI	Asp 110, Ser 192, Ser 196, Thr 115	Val 111, Ile 183, Trp 342, Phe 346, Tyr 373, Thr 369.	*ND	*ND

*ND = Not Determined.
Residues involved in H-Bonds are underlined.
doi:10.1371/journal.pone.0044316.t003

Discussion

In the present study we have successfully modeled and optimized the structure of two high homologous GPCRs, the hD_3 and hD_{2L} receptors. The homology modeling is a powerful tool in the prediction of protein structure. The strength of this methodology is related to the sequence identity shared between the target and the template protein: the highest sequence identity determines the best structure model. We built and validated the homology models of hD_3 and hD_{2L} receptor using the x-ray structure of hD_3 receptor, a lysozyme-chimera protein. The high sequence identity shared by these two receptors did not allow us to differentiate their homology models that were therefore unsuitable for prediction of binding energies and subtype selectivity of D_2-like ligands. The high structure similarity of hD_3 and hD_{2L} arises from the energy minimization process, and represents a weakness in the homology modeling approach. Usually, in homology modeling, the energy optimization of the modeled protein structure is performed by energy minimization *in vacuo*, with some exceptions such as the GPCRRD server http:/zhanglab.ccmb.umich.edu/

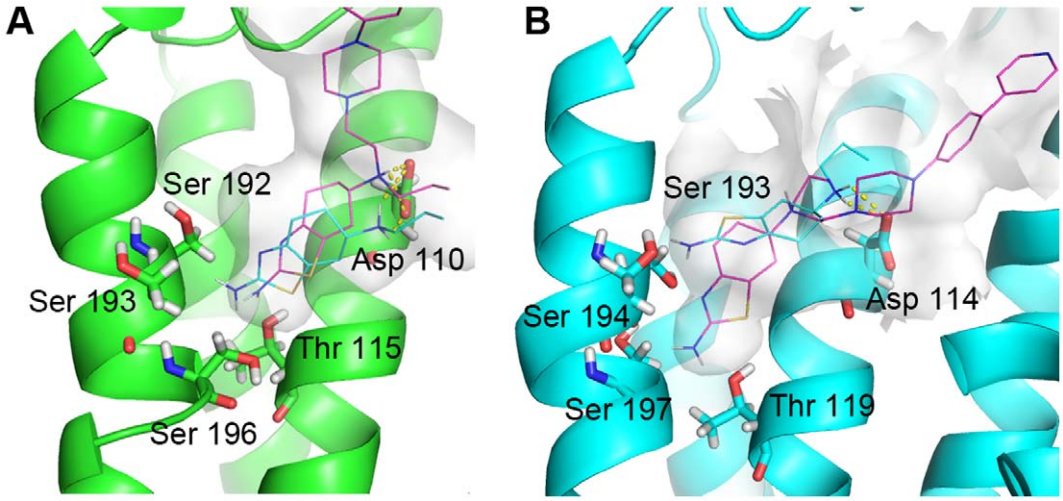

Figure 8. Virtual screening. Pose of pramipexole (cyan lines) and compound ZINC45254546 (magenta lines, see also text) docked into hD_3 (A) and hD_{2L} (B) optimized receptor structures. H-bonds with Aspartate conserved residues are represented with yellow dashes.
doi:10.1371/journal.pone.0044316.g008

Table 4. Virtual Screening. Top scored compound ZINC45254546.

	hD_3	hD_{2L}
Vina (Kcal/mol)	−8.7	−8.1
AD4.2 (Kcal/mol)	−8.8	−7.98
Exp. Ki (nM)	4.78	270
H-bonds and Polar contacts	Asp 110, Thr 115, Ser 196, Ser 182,	Ser 197, Ser 193, Thr 119
Hydrophobic interactions	Val 111, Ile 183, Phe 345, Phe 346, His 349, Tyr 365, Pro 362,Thr 369.	Leu 94, Val 91, Val 111, Ile 184, Val 115, Phe 198, Phe 389, Phe 390, His 393, Thr 412, Tyr 416.

Residues involved in H-bonds are underlined.
doi:10.1371/journal.pone.0044316.t004

GPCRRD/. GPCRRD carries out a pipeline of structural optimizations of homology models, with a final MD simulation: Fragment-Guided Molecular Dynamics (FD-MD), which takes into account knowledge-based (H-bonds and positional restraints) and physics-based atomic potentials (AMBER99 forcefield) [58,59]. So far protein-lipid and protein-water explicit interactions, based on empirical physics-based atomic potentials, are not taken into account by homology modeling software. Thus, we attempted to optimize the structure of the hD_3 and hD_{2L} models by MD in an explicit water-membrane environment, reaching a local conformational minimum within 3 ns. The MD simulations led to structural adaptation and differentiation of the two receptors in membrane, enabling the prediction of trends of pK_i values and the modeling of ligand-protein interactions of D_3-preferring receptor agonists. Moreover, the refined models were useful in the identification, by a virtual screening approach, of an agonist (ZINC45254546) referred to be selective for D_3 over D_2 [57]. Our results are consistent with the findings of Chien et al [26]; the hD_3 homology model we built was validated by docking eticlopride and by obtaining with AD 4.2 a pose highly similar to the one in the x-ray structure 3PBL. Because the ionic lock, a marker of inactive state described in 3PBL, was retained during MD simulations in both hD_3 and hD_{2L} receptors, we can assume that refined models represent an inactive state of the receptors. Moreover, we modeled both disulfide bridges solved in 3PBL in hD_3 model and we modeled just one disulfide bridge, the canonical one, in hD_{2L}. We made this choice because the conserved cysteine residues in the 3ECL, Cys 399 and Cys 401, are separated just by one residue Asp 400, leading to a high constrained loop in the case a disulfide bridge is formed. The lack of the accessory disulfide bridge in the 3ECL might have influenced the dynamics of hD_{2L} receptor, leading to the swelling of its binding pocket, in comparison to the hD_3 which is restrained by two disulfide bridges. Wang et al [60] have predicted the structural differences of hD_3 and hD_2 receptors. The homology models of these GPCRs were built in complex with haloperidol (previously aligned to the β_2-adrenergic inverse agonist s-carazolol), using the crystal structure of β_2-adrenergic receptor (2RH1); the complexes were subsequently simulated in a POPC bilayer for 1.5 ns. Haloperidol in complex with simulated D_3 and D_2 receptors was also used to carry out 3D-QSAR studies using 163 compounds. These authors [35] concluded that the higher affinity of bigger ligands for D_3 receptor over D_2 subtype is related to the shape of binding pocket, which is shallower in D_2 receptor. We found that the binding pocket of hD_3 receptor, after adapting in the membrane environment, significantly deviates from the initial homology model, becoming smaller and partitioned. The binding pocket of hD_3 in membrane environment is also smaller than the one of hD_{2L} receptor. We carried out docking calculations rather than 3D-QSAR (ligand-based method) because we considered our refined models highly predictive due to the crystal structure of hD_3 receptor, used as template for homology modeling. Docking calculations (structure-based method) are strictly related to the reliability of the receptor structure, and we obtained a good correlation of experimental and computed K_i values for agonists docked into hD_3 and hD_{2L} binding sites. Although the prediction of absolute K_i values is a difficult task, AD 4.2 was a powerful tool in order to validate homology model of hD_3 receptor (eticlopride re-docking) as well as to validate the refined models by MD simulations. In fact, the predicted trend of K_i values is well correlated (high Pearson coefficients) with the experimental trend. This correlation was carried out with aminotetraline derivatives, a congeneric chemical class that does not include quinpirole. This latter is a preferential D_3 agonist, but behaved as an outlier in the chemical space of docked ligands, due to the tricyclic structure and the pyrazole moiety. Neverthless, our optimized models were able to predict the affinity of quinpirole higher for D_3 than for D_{2L} receptor. In conclusion, the computational approach, totally structure-based, adopted in the present study is able to build and refine structure models of homologous dopamine receptors that may be of interest for structure-based drug discovery of selective dopaminergic ligands, potentially useful to treat neurological, psychiatric and ocular disorders.

Supporting Information

Supporting Information S1 Figure S1: Energy plots of systems. Potential energy (E_{pot}) and total energy (E_{tot}), of hD_{2L} and hD_3 receptors. Table S1: Cα deviations of transmembrane helices (TM) of D_3 and D_{2L} simulated receptors from the starting models. Cα deviation values were determined by structural alignment of each helix of the model and of the optimized structure. Figure S2: Deviation of helices of optimized hD_{2L} receptor (cyan cartoon) respect the starting model (yellow cartoon). The upper side of the figure corresponds to the extracellular side. Table S2: Computed pK_i for ligands docked into hD3 and hD2L receptors. Values are reported for ligands inserted in the regressions represented in Figure 7. Figure S3: Superimposition of template (3PBL)-homology model- optimized model of hD_3 receptor and hD_{2L} receptor. The template structure (green cartoon) is the A chain of hD_3 receptor crystal structure (3BPL). The cyan cartoon corresponds to the homology model of hD_3 receptor, the yellow cartoon corresponds to the homology model of hD_{2L} receptor. The optimized models of hD3 and hD2L receptor are respectively the magenta and orange cartoons.
(DOCX)

Supporting Information S2 Supplemental files (.pdb files) contained in the compressed directory File S2 include poses of

ligands, shown in Figure 1, docked into hD_3 and hD_{2L} optimized receptors, whose.pdb files are also included in File S2. All.pdb files can be visualized with Open Pymol. Files named ligand_D2.pdb correspond to poses of ligand docked into hD_{2L} receptor, whereas files named ligand_D3.pdb correspond to poses into hD_3 receptor. The optimized structure of hD3 and hD2L receptor are named respectively opt_D3_receptor.pdb and opt_D2L_receptor.
(ZIP)

Author Contributions

Conceived and designed the experiments: CBMP CB GML. Performed the experiments: CBMP. Analyzed the data: CBMP CB SS. Contributed reagents/materials/analysis tools: CBMP CB. Wrote the paper: CBMP CB GML SS FD.

References

1. Beaulieu JM, Gainetdinov RR (2011) The physiology, signaling, and pharmacology of dopamine receptors. Pharmacological reviews 63: 182–217.
2. Lindgren N, Usiello A, Goiny M, Haycock J, Erbs E, et al. (2003) Distinct roles of dopamine D2L and D2S receptor isoforms in the regulation of protein phosphorylation at presynaptic and postsynaptic sites. Proc Natl Acad Sci U S A 100: 4305–4309.
3. Landwehrmeyer B, Mengod G, Palacios JM (1993) Dopamine D3 receptor mRNA and binding sites in human brain. Brain Res Mol Brain Res 18: 187–192.
4. Diaz J, Pilon C, Le Foll B, Gros C, Triller A, et al. (2000) Dopamine D3 receptors expressed by all mesencephalic dopamine neurons. J Neurosci 20: 8677–8684.
5. Chen PC, Lao CL, Chen JC (2009) The D(3) dopamine receptor inhibits dopamine release in PC-12/hD3 cells by autoreceptor signaling via PP-2B, CK1, and Cdk-5. J Neurochem 110: 1180–1190.
6. Ballesteros JA, Shi L, Javitch JA (2001) Structural mimicry in G protein-coupled receptors: implications of the high-resolution structure of rhodopsin for structure-function analysis of rhodopsin-like receptors. Mol Pharmacol 60: 1–19.
7. Neve KA, Seamans JK, Trantham-Davidson H (2004) Dopamine receptor signaling. J Recept Signal Transduct Res 24: 165–205.
8. Sokoloff P, Diaz J, Le Foll B, Guillin O, Leriche L, et al. (2006) The dopamine D3 receptor: a therapeutic target for the treatment of neuropsychiatric disorders. CNS Neurol Disord Drug Targets 5: 25–43.
9. Potter DE, Ogidigben MJ, Chu TC (1998) Lisuride acts at multiple sites to induce ocular hypotension and mydriasis. Pharmacology 57: 249–260.
10. Ogidigben M, Chu TC, Potter DE (1993) Ocular hypotensive action of a dopaminergic (DA2) agonist, 2,10,11-trihydroxy-N-n-propylnoraporphine. The Journal of pharmacology and experimental therapeutics 267: 822–827.
11. Potter DE, Shumate DJ (1987) Cianergoline lowers intraocular pressure in rabbits and monkeys and inhibits contraction of the cat nictitans by suppressing sympathetic neuronal function. Journal of ocular pharmacology 3: 309–321.
12. Mekki QA, Hassan SM, Turner P (1983) Bromocriptine lowers intraocular pressure without affecting blood pressure. Lancet 1: 1250–1251.
13. Geyer O, Robinson D, Lazar M (1987) Hypotensive effect of bromocriptine in glaucomatous eyes. Journal of ocular pharmacology 3: 291–294.
14. Chu E, Chu TC, Potter DE (2000) Mechanisms and sites of ocular action of 7-hydroxy-2-dipropylaminotetralin: a dopamine(3) receptor agonist. J Pharmacol Exp Ther 293: 710–716.
15. Bucolo C, Leggio GM, Maltese A, Castorina A, D'Agata V, et al. (2011) Dopamine-3 receptor modulates intraocular pressure: implications for glaucoma. Biochem Pharmacol 83: 680–686.
16. Sibley DR, Monsma FJ Jr (1992) Molecular biology of dopamine receptors. Trends Pharmacol Sci 13: 61–69.
17. Levant B (1997) The D3 dopamine receptor: neurobiology and potential clinical relevance. Pharmacol Rev 49: 231–252.
18. Sokoloff P, Giros B, Martres MP, Bouthenet ML, Schwartz JC (1990) Molecular cloning and characterization of a novel dopamine receptor (D3) as a target for neuroleptics. Nature 347: 146–151.
19. Shi L, Javitch JA (2002) The binding site of aminergic G protein-coupled receptors: the transmembrane segments and second extracellular loop. Annu Rev Pharmacol Toxicol 42: 437–467.
20. Malmberg A, Nordvall G, Johansson AM, Mohell N, Hacksell U (1994) Molecular basis for the binding of 2-aminotetralins to human dopamine D2A and D3 receptors. Mol Pharmacol 46: 299–312.
21. Chumpradit S, Kung MP, Kung HF (1993) Synthesis and optical resolution of (R)- and (S)-trans-7-Hydroxy-2-[N-propyl-N-(3′-iodo-2′-propenyl)amino]tetralin: a new D3 dopamine receptor ligand. J Med Chem 36: 4308–4312.
22. Chumpradit S, Kung MP, Vessotskie J, Foulon C, Mu M, et al. (1994) Iodinated 2-aminotetralins and 3-amino-1-benzopyrans: ligands for dopamine D2 and D3 receptors. J Med Chem 37: 4245–4250.
23. Martin PL, Kelly M, Cusack NJ (1993) (-)-2-(N-propyl-N-2-thienylethylamino)-5-hydroxytetralin (N-0923), a selective D2 dopamine receptor agonist demonstrates the presence of D2 dopamine receptors in the mouse vas deferens but not in the rat vas deferens. J Pharmacol Exp Ther 267: 1342–1348.
24. Reynolds NA, Wellington K, Easthope SE (2005) Rotigotine: in Parkinson's disease. CNS drugs 19: 973–981.
25. Glase SA, Corbin AE, Pugsley TA, Heffner TG, Wise LD (1995) Synthesis and dopaminergic activity of pyridine analogs of 5-hydroxy-2-(di-n-propylamino)tetralin. J Med Chem 38: 3132–3137.
26. Mierau J, Schneider FJ, Ensinger HA, Chio CL, Lajiness ME, et al. (1995) Pramipexole binding and activation of cloned and expressed dopamine D2, D3 and D4 receptors. Eur J Pharmacol 290: 29–36.
27. Bettinetti L, Schlotter K, Hubner H, Gmeiner P (2002) Interactive SAR studies: rational discovery of super-potent and highly selective dopamine D3 receptor antagonists and partial agonists. J Med Chem 45: 4594–4597.
28. Lopez L, Selent J, Ortega R, Masaguer CF, Dominguez E, et al. (2010) Synthesis, 3D-QSAR, and structural modeling of benzolactam derivatives with binding affinity for the D(2) and D(3) receptors. ChemMedChem 5: 1300–1317.
29. Ortega R, Hubner H, Gmeiner P, Masaguer CF (2011) Aromatic ring functionalization of benzolactam derivatives: new potent dopamine D3 receptor ligands. Bioorganic & medicinal chemistry letters 21: 2670–2674.
30. Tschammer N, Elsner J, Goetz A, Ehrlich K, Schuster S, et al. (2011) Highly potent 5-aminotetrahydropyrazolopyridines: enantioselective dopamine D3 receptor binding, functional selectivity, and analysis of receptor-ligand interactions. J Med Chem 54: 2477–2491.
31. Chien EY, Liu W, Zhao Q, Katritch V, Han GW, et al. (2010) Structure of the human dopamine D3 receptor in complex with a D2/D3 selective antagonist. Science 330: 1091–1095.
32. Carlsson J, Coleman RG, Setola V, Irwin JJ, Fan H, et al. (2011) Ligand discovery from a dopamine D3 receptor homology model and crystal structure. Nat Chem Biol 7: 769–778.
33. Obiol-Pardo C, Lopez L, Pastor M, Selent J (2011) Progress in the structural prediction of G protein-coupled receptors: D3 receptor in complex with eticlopride. Proteins 79: 1695–1703.
34. Kortagere S, Cheng SY, Antonio T, Zhen J, Reith ME, et al. (2011) Interaction of novel hybrid compounds with the D3 dopamine receptor: Site-directed mutagenesis and homology modeling studies. Biochemical pharmacology 81: 157–163.
35. Wang Q, Mach RH, Luedtke RR, Reichert DE (2010) Subtype selectivity of dopamine receptor ligands: insights from structure and ligand-based methods. Journal of chemical information and modeling 50: 1970–1985.
36. Arnold K, Bordoli L, Kopp J, Schwede T (2006) The SWISS-MODEL workspace: a web-based environment for protein structure homology modelling. Bioinformatics 22: 195–201.
37. Kiefer F, Arnold K, Kunzli M, Bordoli L, Schwede T (2009) The SWISS-MODEL Repository and associated resources. Nucleic Acids Res 37: D387–392.
38. Humphrey W, Dalke A, Schulten K (1996) VMD: visual molecular dynamics. J Mol Graph 14: 33–38, 27–38.
39. Phillips JC, Braun R, Wang W, Gumbart J, Tajkhorshid E, et al. (2005) Scalable molecular dynamics with NAMD. J Comput Chem 26: 1781–1802.
40. Darden T YD, Pedersen L (1993) Particle mesh Ewald: An N [center-dot] log(N) method for Ewald sums in large systems. J Chem Phys 98: 10089–10092.
41. Trott O, Olson AJ (2010) AutoDock Vina: improving the speed and accuracy of docking with a new scoring function, efficient optimization, and multithreading. J Comput Chem 31: 455–461.
42. Morris GM, Goodsell DS, Huey R, Olson AJ (1996) Distributed automated docking of flexible ligands to proteins: parallel applications of AutoDock 2.4. J Comput Aided Mol Des 10: 293–304.
43. Huey R, Morris GM, Olson AJ, Goodsell DS (2007) A semiempirical free energy force field with charge-based desolvation. J Comput Chem 28: 1145–1152.
44. Sayers EW, Barrett T, Benson DA, Bolton E, Bryant SH, et al. (2012) Database resources of the National Center for Biotechnology Information. Nucleic Acids Res 40: D13–25.
45. Irwin JJ, Shoichet BK (2005) ZINC–a free database of commercially available compounds for virtual screening. J Chem Inf Model 45: 177–182.
46. Schuttelkopf AW, van Aalten DM (2004) PRODRG: a tool for high-throughput crystallography of protein-ligand complexes. Acta Crystallogr D Biol Crystallogr 60: 1355–1363.
47. O'Boyle NM, Banck M, James CA, Morley C, Vandermeersch T, et al. (2011) Open Babel: An open chemical toolbox. J Cheminform 3: 33.
48. Ballesteros JA, Jensen AD, Liapakis G, Rasmussen SG, Shi L, et al. (2001) Activation of the beta 2-adrenergic receptor involves disruption of an ionic lock between the cytoplasmic ends of transmembrane segments 3 and 6. The Journal of biological chemistry 276: 29171–29177.
49. Okada T, Sugihara M, Bondar AN, Elstner M, Entel P, et al. (2004) The retinal conformation and its environment in rhodopsin in light of a new 2.2 A crystal structure. Journal of molecular biology 342: 571–583.

50. Palczewski K, Kumasaka T, Hori T, Behnke CA, Motoshima H, et al. (2000) Crystal structure of rhodopsin: A G protein-coupled receptor. Science 289: 739–745.
51. Vogel R, Mahalingam M, Ludeke S, Huber T, Siebert F, et al. (2008) Functional role of the ''ionic lock''–an interhelical hydrogen-bond network in family A heptahelical receptors. Journal of molecular biology 380: 648–655.
52. Le Guilloux V, Schmidtke P, Tuffery P (2009) Fpocket: an open source platform for ligand pocket detection. BMC bioinformatics 10: 168.
53. Yap BK, Buckle MJ, Doughty SW (2012) Homology modeling of the human 5-HT(1A), 5-HT (2A), D1, and D2 receptors: model refinement with molecular dynamics simulations and docking evaluation. Journal of molecular modeling.
54. Lape M, Elam C, Paula S (2010) Comparison of current docking tools for the simulation of inhibitor binding by the transmembrane domain of the sarco/endoplasmic reticulum calcium ATPase. Biophys Chem 150: 88–97.
55. Yap BK, Buckle MJ, Doughty SW (2012) Homology modeling of the human 5-HT(1A), 5-HT (2A), D1, and D2 receptors: model refinement with molecular dynamics simulations and docking evaluation. J Mol Model.
56. Kuzhikandathil EV, Kortagere S (2012) Identification and Characterization of a Novel Class of Atypical Dopamine Receptor Agonists. Pharmaceutical research.
57. Ghosh B, Antonio T, Zhen J, Kharkar P, Reith ME, et al. (2010) Development of (S)-N6-(2-(4-(isoquinolin-1-yl)piperazin-1-yl)ethyl)-N6-propyl-4,5,6,7-tetrahydro benzo[d]-thiazole-2,6-diamine and its analogue as a D3 receptor preferring agonist: potent in vivo activity in Parkinson's disease animal models. J Med Chem 53: 1023–1037.
58. Zhang J, Zhang Y (2010) GPCRRD: G protein-coupled receptor spatial restraint database for 3D structure modeling and function annotation. Bioinformatics 26: 3004–3005.
59. Zhang J, Liang Y, Zhang Y (2011) Atomic-level protein structure refinement using fragment-guided molecular dynamics conformation sampling. Structure 19: 1784–1795.
60. Wang Q, Mach RH, Luedtke RR, Reichert DE (2010) Subtype selectivity of dopamine receptor ligands: insights from structure and ligand-based methods. J Chem Inf Model 50: 1970–1985.
61. Millan MJ, Newman-Tancredi A, Audinot V, Cussac D, Lejeune F, et al. (2000) Agonist and antagonist actions of yohimbine as compared to fluparoxan at alpha(2)-adrenergic receptors (AR)s, serotonin (5-HT)(1A), 5-HT(1B), 5-HT(1D) and dopamine D(2) and D(3) receptors. Significance for the modulation of frontocortical monoaminergic transmission and depressive states. Synapse 35: 79–95.
62. Millan MJ, Maiofiss L, Cussac D, Audinot V, Boutin JA, et al. (2002) Differential actions of antiparkinson agents at multiple classes of monoaminergic receptor. I. A multivariate analysis of the binding profiles of 14 drugs at 21 native and cloned human receptor subtypes. The Journal of pharmacology and experimental therapeutics 303: 791–804.
63. Scheller D, Ullmer C, Berkels R, Gwarek M, Lubbert H (2009) The in vitro receptor profile of rotigotine: a new agent for the treatment of Parkinson's disease. Naunyn-Schmiedeberg's archives of pharmacology 379: 73–86.
64. Sokoloff P, Andrieux M, Besancon R, Pilon C, Martres MP, et al. (1992) Pharmacology of human dopamine D3 receptor expressed in a mammalian cell line: comparison with D2 receptor. European journal of pharmacology 225: 331–337.
65. Tadori Y, Forbes RA, McQuade RD, Kikuchi T (2011) Functional potencies of dopamine agonists and antagonists at human dopamine D(2) and D(3) receptors. European journal of pharmacology 666: 43–52.
66. Scheideler MA, Martin J, Hohlweg R, Rasmussen JS, Naerum L, et al. (1997) The preferential dopamine D3 receptor agonist cis-8-OH-PBZI induces limbic Fos expression in rat brain. European journal of pharmacology 339: 261–270.